

# A novel tool for rapid optimization of stationary tokamak plasmas using RAPTOR-QLKNN applied to the ITER hybrid scenario

S Van Mulders<sup>1</sup>, F Felici<sup>1</sup>, O Sauter<sup>1</sup>, J Citrin<sup>2</sup>, A Ho<sup>2</sup>, M Marin<sup>2</sup> and K L van de Plassche<sup>2</sup>

<sup>1</sup> *Ecole Polytechnique Fédérale de Lausanne (EPFL), Swiss Plasma Center (SPC), CH-1015 Lausanne, Switzerland*

<sup>2</sup> *Dutch Institute for Fundamental Energy Research (DIFFER), PO Box 6336, 5600 HH Eindhoven, The Netherlands*

**Abstract** This work presents a framework for fast, automated optimization of the stationary phase of tokamak plasma discharges and its application to first-principle-based modeling of the ITER hybrid scenario [1].

**Introduction and framework set-up** The RAPTOR fast transport solver [2] is extended with a new solution method allowing to directly obtain the stationary solution of the coupled, non-linear diffusion equations for ion and electron temperature and density and current density. Coupled to QLKNN-hyper-10D [3], a neural network emulation of the quasi-linear gyrokinetic QuaLiKiz transport model [4], a first-principle-based estimate of the stationary state of the core plasma can be found at unprecedented computational speed (typically a few seconds on standard hardware).

The stationary state solver is embedded in a numerical optimization scheme, accelerating the optimization of tokamak plasma scenarios and guiding the efforts of more extensive integrated modeling tools. The optimization scheme profits from the availability of analytic Jacobians in RAPTOR.

Iterative application of the stationary state solver and the CHEASE fixed boundary equilibrium solver [5] allows to assess the impact of the MHD equilibrium on the resulting stationary plasma profiles. A moderate impact of MHD equilibrium consistency allows the optimization routine to scan over different operational scenarios, without need for updating the equilibrium geometry.

The fast computational time allows for applications in scenario design, inter-discharge optimization and system codes.

**Application for ITER hybrid scenario** For the ITER hybrid results shown here, the stationary solution is calculated for electron and ion heat transport and current diffusion, while a density profile is imposed with Greenwald fraction  $f_{Gw} = 0.9$  and moderate density peaking  $n_0/n_{ped} = 1.4$ . A temperature pedestal of 4.5 keV is imposed at  $\rho_{tor} = 0.9$ , while the density pedestal is linearly increasing with  $I_p$ , consistent with the pedestal pressure scaling law presented in [6]. Auxiliary heating is provided by 33 MW of neutral beam injection and up to 40 MW of electron cyclotron heating. Thermal diffusivities are predicted by the QLKNN surrogate model based on 10 local plasma quantities and are dominated by ITG-driven turbulence.

The present simulations do not take into account the magnetic flux pumping effect and rely on off-axis

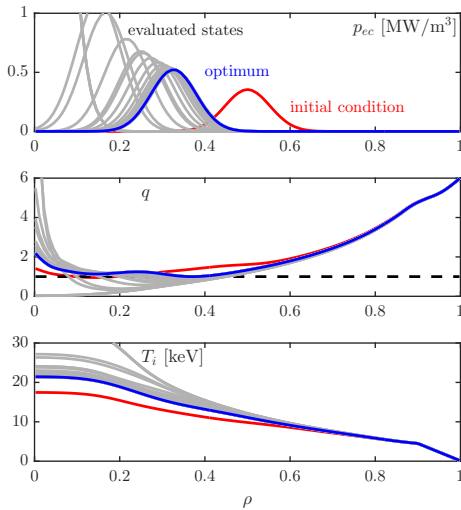


Figure 1: Heat deposition  $p_{ec}$ ,  $q$  and  $T_i$  profiles for every stationary plasma state visited by the optimization routine

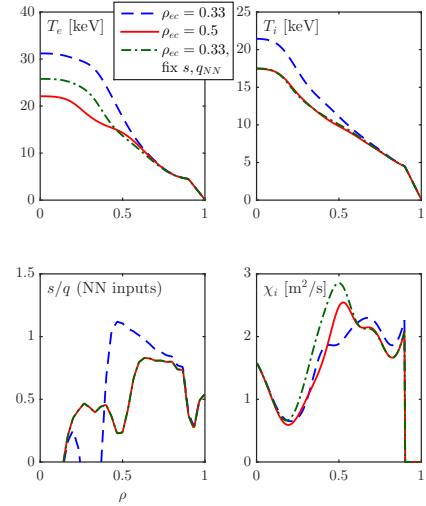


Figure 2: Stationary state for:  $\rho_{ec} = 0.5$  (red);  $\rho_{ec} = 0.33$  (blue);  $\rho_{ec} = 0.33$  with  $s, q$  profiles of the  $\rho_{ec} = 0.5$  simulation to the NN inputs (green)

electron cyclotron current drive (ECCD) to shape the  $q$  profile, to maximize confinement and maintain  $q > 1$ . Figure 1 illustrates the different stationary state evaluations requested by the non-linear optimizer when searching for the optimum ECCD deposition radius, assuming a gaussian deposition profile with width  $\Delta\rho = 0.15$  and 40MW of injected power (with a current drive efficiency proportional to  $T_e/n_e$ ). Figure 2 shows that shifting the deposition radius closer to the magnetic axis, an increase of  $s/q$  is obtained at outer radii in the core, impacting the ITG threshold and leading to a rise of  $T_i$ . To maximize the fusion power, the current has to be driven as close to axis as possible while satisfying the constraint  $q > 1$ .

For a given amount of injected auxiliary power, both fusion power  $P_{fus}$  and fusion gain  $Q$  increase when increasing plasma current  $I_p$ , while maintaining the fraction of the line-averaged density to the Greenwald density limit constant. The maximum plasma current for which  $q > 1$  can be maintained is dependent on both the available amount of electron cyclotron power and the plasma density, as both impact the amount of off-axis current drive that can be deposited to tailor the  $q$  profile, as illustrated in Figure 3, giving a quantitative assessment of the scenarios that can be achieved with respectively  $P_{ec} = 20$  and 40 MW.

Due to the stiffness of the QLKNN-predicted transport, an increase of fusion gain can be achieved by reducing the electron cyclotron power, with the magnitude of the increase of  $Q$  dependent on the feasible reduction of  $P_{ec}$ , as illustrated in Figure 4. An additional constraint is added to ensure that the power crossing the separatrix  $P_{sep}$  remains more than 20% in excess of the HL threshold power  $P_{LH}$ :  $P_{sep} > 1.2P_{LH}$ . Depending on the level of the plasma current, the reduction of  $P_{ec}$  is limited by one of the following constraints:

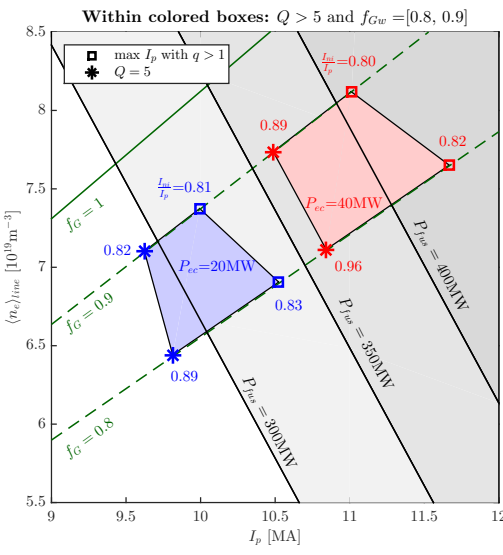


Figure 3:  $Q > 5$ ,  $f_{Gw} = [0.8, 0.9]$  operating window for  $P_{ec} = 20$  (blue) or  $40$  MW (red)

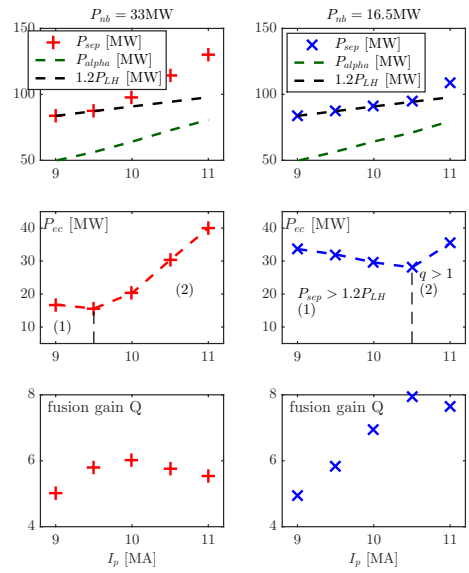


Figure 4: Operating points maximizing  $Q$  by optimizing  $\rho_{ec}$  and  $P_{ec}$  with  $q > 1$  and  $P_{sep} > 1.2P_{LH}$

- The current density profiles of scenarios at the *higher end of the  $I_p$  range* have a comparatively larger contribution driven inductively and hence require in absolute terms more off-axis non-inductive current drive to maintain  $q > 1$ , limiting the feasible  $P_{ec}$  reduction. Since this effect dominates the increase of fusion power for increased plasma current (due to increased density), *an increase of  $I_p$  leads to a decreasing fusion gain  $Q$ .*
- For scenarios at the *lower end of the  $I_p$  range* the feasible reduction of the electron cyclotron power is limited by the  $P_{LH}$  constraint. This is clearly illustrated in the upper panels of Figure 4, where the power crossing the separatrix and the constraining lower value are shown for the different scenarios. Although the required threshold power  $P_{LH}$  decreases for reduced plasma current  $I_p$  (due to reduced density), this does not lead to a reduction of the required total auxiliary power since fusion power is essentially proportional to the square of the density and the plasma self-heating due to fusion-born alphas hence strongly diminishes (also shown in Figure 4). Within this range, *an increase of  $I_p$  allows for an increasing fusion gain  $Q$ .*

Due to these counteracting considerations, the achievable increase for the fusion gain  $Q$  is most pronounced for intermediate plasma currents.

**Iterative scheme with CHEASE MHD equilibrium solver** The mutual dependence of the transport equations on geometric equilibrium quantities and of the Grad-Shafranov equation on radial transport profiles demand an integrated approach to achieve full consistency. To assess the impact of the underlying MHD equilibrium on the transport solutions, an automatic interfacing between RAPTOR and CHEASE was implemented, allowing to iteratively approach a consistent set of equilibrium and pro-

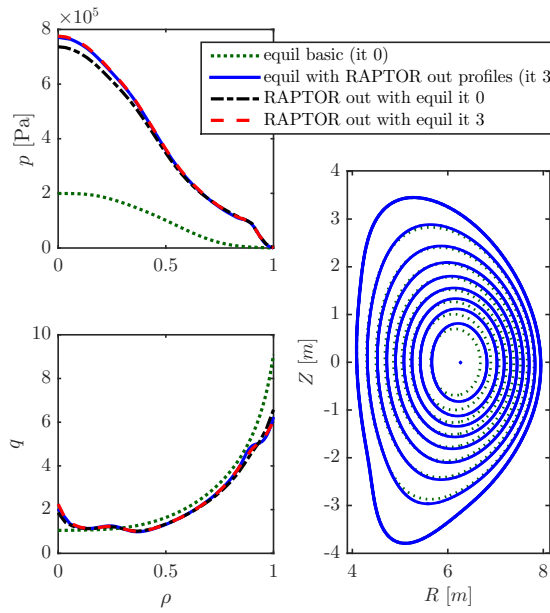


Figure 5: Impact of MHD equilibrium consistency on transport solution (magnetic surfaces are shown for both equilibria for 10 equidistant values of the normalized poloidal flux)

files. To illustrate this procedure, a basic MHD equilibrium was constructed in CHEASE, assuming simple radial profiles (shown in green dotted on Figure 5). After three RAPTOR-CHEASE iterations, the RAPTOR transport solution converges towards the profiles underlying the CHEASE equilibrium. From Figure 5 it is clear that even for a large equilibrium change, the impact on the transport solution is moderate. As a consequence, it is well justified to avoid equilibrium updates during the iterations of the optimizer and only use the final optimized profiles to obtain the consistent equilibria.

**Conclusion** Predictive modeling tools are often applied to explore the existence of stationary scenarios for current and future devices. The work shown in this contribution has the potential to substantially reduce the effort of such modeling activities by calculating stationary states directly (without requiring iteration between several codes) and allowing the use of numerical optimization tools to find optimal scenarios satisfying constraints. These can then serve as starting point for more sophisticated analysis using more detailed physics codes.

This work has been carried out within the framework of the EUROfusion Consortium and has received funding from the Euratom research and training programme 2014-2018 and 2019-2020 under grant agreement No 633053. The views and opinions expressed herein do not necessarily reflect those of the European Commission. This work was supported in part by the Swiss National Science Foundation.

## References

- [1] S Van Mulders *et al* Accepted by *Nucl. Fusion*
- [2] F Felici *et al* 2012 *Plasma Phys. Control. Fusion* **54** 025002
- [3] K L van de Plassche *et al* 2020 *Phys. Plasmas* **27** 025002
- [4] C Bourdelle *et al* 2016 *Plasma Phys. Control. Fusion* **58** 014036
- [5] H Lütjens *et al* 1996 *Comput. Phys. Commun.* **97** 219
- [6] A R Polevoi *et al* 2015 *Nucl. Fusion* **55** 063019